

- 1998, 2249–2250; e) J. Renaud, C.-D. Graf, L. Oberer, *Angew. Chem.* **2000**, *112*, 3231–3234; *Angew. Chem. Int. Ed.* **2000**, *39*, 3101–3104, and references therein.
- [5] S.-H. Kim, W. J. Zuercher, N. B. Bowden, R. H. Grubbs, *J. Org. Chem.* **1996**, *61*, 1073–1081.
- [6] E. M. Codesido, L. Castedo, J. R. Granja, *Org. Lett.* **2001**, *3*, 1483–1486.
- [7] F.-D. Boyer, I. Hanna, L. Ricard, *Org. Lett.* **2001**, *3*, 3095–3098.
- [8] For pioneering work with platinum complexes, see: a) B. M. Trost, V. K. Chang, *Synthesis* **1993**, 824–832; b) J. Blum, H. Beer-Kraft, Y. Badrieh, *J. Org. Chem.* **1995**, *60*, 5567–5569; see also: c) B. M. Trost, G. A. Doherty, *J. Am. Chem. Soc.* **2000**, *122*, 3801–3810.
- [9] a) N. Chatani, N. Furukawa, H. Sakurai, S. Murai, *Organometallics* **1996**, *15*, 901–903; b) A. Fürstner, H. Szillat, B. Gabor, R. Mynott, *J. Am. Chem. Soc.* **1998**, *120*, 8305–8314; c) A. Fürstner, H. Szillat, F. Stelzer, *J. Am. Chem. Soc.* **2000**, *122*, 6785–6786; d) A. Fürstner, F. Stelzer, H. Szillat, *J. Am. Chem. Soc.* **2001**, *123*, 11863–11869.
- [10] For studies on a linear dienyne system, see: N. Chatani, K. Kataoka, S. Murai, N. Furukawa, Y. Seki, *J. Am. Chem. Soc.* **1998**, *120*, 9104–9105.
- [11] For reactions with external trapping, see: a) M. Méndez, M. P. Muñoz, A. M. Echavarren, *J. Am. Chem. Soc.* **2000**, *122*, 11549–11550; b) M. Méndez, M. P. Muñoz, C. Nevado, D. J. Cárdenas, A. M. Echavarren, *J. Am. Chem. Soc.* **2001**, *123*, 10511–10520.
- [12] CCDC-172245 contains the supplementary crystallographic data for compound **3e**. These data can be obtained free of charge via www.ccdc.cam.ac.uk/conts/retrieving.html (or from the Cambridge Crystallographic Data Centre, 12, Union Road, Cambridge CB2 1EZ, UK; fax: (+44) 1223-336-033; or deposit@ccdc.cam.ac.uk).
- [13] For a related formation of a tetracyclic derivative with two cyclopropyl rings from a linear dienyne precursor, see ref. [10].
- [14] For further mechanistic data, see: a) N. Chatani, H. Inoue, T. Ikeda, S. Murai, *J. Org. Chem.* **2000**, *65*, 4913–4918; b) S. Oi, I. Tsukamoto, S. Miyano, Y. Inoue, *Organometallics* **2001**, *20*, 3704–3709.
- [15] The stereochemical assignment was deduced from NOESY studies.
- [16] M. H. Chisholm, H. C. Clark, *Acc. Chem. Res.* **1973**, *6*, 202–209.
- [17] For such an intermediate with Ru^{II} complexes, see: D. Pilette, S. Moreau, H. Le Bozec, P. H. Dixneuf, J. F. Corrigan, A. J. Carty, *Chem. Commun.* **1994**, 409–410.
- [18] G. Mehta, V. Singh, *Chem. Rev.* **1999**, *99*, 881–930.
- [19] a) A. Padwa, K. E. Krumpe, *Tetrahedron* **1992**, *48*, 5385–5453; b) T. Ye, A. McKervy, *Chem. Rev.* **1994**, *94*, 1091–1160; c) M. P. Doyle in *Comprehensive Organometallic Chemistry*, Vol. 12 (Eds.: E. W. Abel, F. G. A. Stone, G. Wilkinson, L. Hegedus), Pergamon, Oxford, **1995**, pp. 387–420.
- [20] a) H.-U. Reißig in *The Chemistry of the Cyclopropyl Group* (Eds.: S. Patai, Z. Rappoport), Wiley, Chichester, **1987**, pp. 375–443; b) J. Salaün in *The Chemistry of the Cyclopropyl Group* (Eds.: S. Patai, Z. Rappoport), Wiley, Chichester, **1987**, pp. 809–878.
- [21] The structural–functional assembly present in adducts **3** is partially incorporated in tricyclic DNA derivatives: R. Steffens, C. J. Leumann, *J. Am. Chem. Soc.* **1999**, *121*, 3249–3255.

Dioxygen Activation by a Mononuclear Ir^{II}–Ethene Complex

Bas de Bruin,* Theo P. J. Peters, Simone Thewissen, Arno N. J. Blok, Jos B. M. Wilting, René de Gelder, Jan M. M. Smits, and Anton W. Gal*

In an attempt to gain a mechanistic insight into the rhodium- and iridium-catalyzed oxygenation of olefins, we have recently investigated stoichiometric oxygenation of N ligand Rh^I– and Ir^I–olefin complexes by O₂ (olefin = ethene, propene, 1,5-cyclooctadiene).^[1, 2]

The reactivity of Rh^I– and Ir^I–ethene fragments towards dioxygen varied between ethene displacement (Figure 1 a), formation of mixed O₂–ethene complexes (Figure 1 b), C–O bond making (giving a 3-metalla(III)–1,2-dioxolane; Figure 1 c), and combined C–O bond making and O–O bond breaking (giving a 2-metalla(III)oxetane; Figure 1 d) The outcome of the oxygenation reaction varies with the N ligand and the central metal.

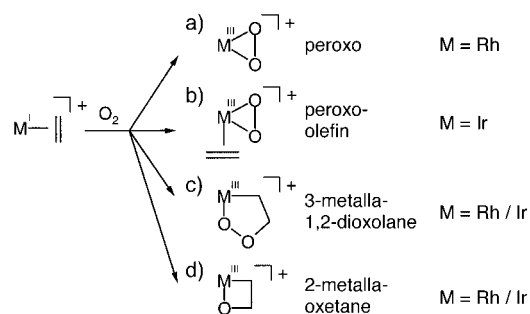


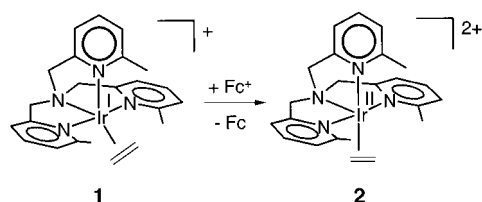
Figure 1. Oxygenation products from the reaction of [(N ligand)M^I(olefin)]⁺ (M = Rh/Ir) complexes with O₂.

Recently, we described the oxygenation of the iridium(II)–ethene complex [(κ⁴-Me₃-tpa)Ir^{II}(C₂H₄)]⁺ (**1**; Me₃-tpa = *N,N,N*-tri((6-methyl-2-pyridyl)methyl)amine) by O₂ to the peroxo–ethene complex [(κ³-Me₃-tpa)Ir^{III}(C₂H₄)(O₂)]⁺ (Figure 1 b) and unidentified paramagnetic species.^[2] We now report the one-electron oxidation of the Ir^I–ethene complex **1** to the unprecedented Ir^{II}–ethene complex [(κ⁴-Me₃-tpa)Ir^{II}(C₂H₄)]²⁺ (**2**; see Scheme 1), and the reactivity of **2** towards O₂.

Treatment of **1**·PF₆ with ferrocenium hexafluorophosphate ([Fc]PF₆) in CH₂Cl₂ resulted in precipitation of **2**·(PF₆)₂ as a brown powder. Thus, one-electron oxidation of Ir^I–ethene complex **1** with Fc⁺ results in the clean formation of the stable Ir^{II}–ethene complex **2** (Scheme 1).

[*] Dr. B. de Bruin, Prof. Dr. A. W. Gal, T. P. J. Peters, S. Thewissen, A. N. J. Blok, J. B. M. Wilting, R. de Gelder, J. M. M. Smits
Department of Inorganic Chemistry
University of Nijmegen
Toernooiveld 1, 6525 ED Nijmegen (The Netherlands)
Fax: (+31) 24-355-3450
E-mail: bdebruin@sci.kun.nl, gal@sci.kun.nl

Supporting information for this article is available on the WWW under <http://www.angewandte.org> or from the author.



Scheme 1. Oxidation of **1** with Fc^+ yielding **2**.

Dark brown crystals of **2**-(PF_6)₂, suitable for X-ray diffraction, were obtained from an acetone solution layered with hexane, at 10 °C. Transparent brown-red crystals of **1**- PF_6 were grown from a CH_2Cl_2 solution layered with hexane, at 4 °C. The structures of both **1** and **2** were determined by single-crystal X-ray diffraction (Figure 2 and Table 1).^[3]

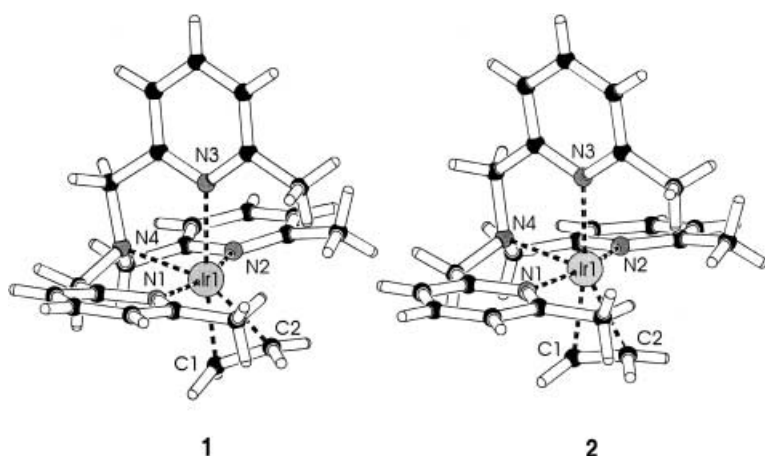


Figure 2. Molecular structure of **1** and **2**.

Table 1. Selected bond lengths [Å] and angles [°] for **1** and **2**.^[a]

	1	2
N1–Ir1	2.075(7)	2.071(5)
N2–Ir1	2.043(8)	2.062(5)
N3–Ir1	2.260(7)	2.136(5)
N4–Ir1	2.154(8)	2.146(5)
C1–Ir1	2.042(9)	2.136(6)
C2–Ir1	2.143(9)	2.149(6)
C1–C2	1.451(13)	1.380(9)
N4–Ir1–C1	109.2(4)	92.4(2)
N4–Ir1–C2	149.5(3)	129.8(2)
N3–Ir1–C1	173.3(3)	172.0(2)
N3–Ir1–C2	132.8(2)	150.2(2)
N3–Ir1–N4	77.4(3)	80.03(17)

[a] For atom labeling see Figure 2.

The structure of **1** is best described as distorted trigonal bipyramidal (*tbp*), with N1 and N2 at the axial positions and N3, N4, and ethene in the equatorial plane. Remarkably, upon one-electron oxidation of **1** to **2**, the coordination geometry changes from *tbp* to distorted square pyramidal (*sqpy*), with N4 at the apical position and N1, N2, N3, and ethene in the basal plane.

Oxidation of **1** to **2** results in a stronger binding of Me_3tpa to the Ir center; the Ir–N3 bond shortens by ~ 0.12 Å, whereas the N1–Ir1, N2–Ir1, and N4–Ir1 bonds do not

significantly change (Table 1). The shortening of the C1–C2 bond by 0.07 Å and the elongation of the Ir–C1 bond by 0.09 Å on going from **1** to **2** indicates weakening of the Ir–ethene interaction upon oxidation of Ir^I to Ir^{II}. Since one cannot imagine a decrease in the ethene \rightarrow Ir σ bonding, the weaker Ir–ethene interaction must result from decreased Ir \rightarrow ethene π backbonding in **2**. In **1**, the Ir1–C2 bond is approximately 0.1 Å longer than the Ir1–C1 bond, probably because the axial Py–Me substituents of the Me_3tpa ligand hinder a closer approach of C2 to the iridium center.

The EPR spectrum of **2** is shown in Figure 3a. Simulation of the rhombic spectrum yielded: $g_{11} = 1.975$, $g_{22} = 2.265$, and $g_{33} = 2.538$. The (super)hyperfine coupling pattern for the g_{11} signal was satisfactorily simulated by assuming hyperfine coupling with the iridium center ($A_{11}^{\text{Ir}} = 129$ MHz) and superhyperfine coupling with one nitrogen atom ($A_{11}^{\text{N}} = 55$ MHz). Contributions from other N nuclei are not resolved in this direction. The g_{22} signal reveals no resolved hyperfine coupling.

The nature of the observed five-line (super)hyperfine coupling pattern of the g_{33} signal is presently not understood. It is satisfactorily simulated by assuming superhyperfine coupling with four (nearly) equivalent $I = 1/2$ nuclei, possibly the four H nuclei of the ethene fragment of **2**. However, the thus obtained superhyperfine coupling constant $A_{33}^{\text{H}} \approx 160$ MHz seems unusually large for hydrogen atoms.^[4] Alternative simulations, which assume coupling with two (nearly) equivalent N nuclei or coupling with one N nucleus and two (nearly) equivalent H nuclei, yield less satisfactory results and still require unusually large superhyperfine coupling constants ($A_{33}^{\text{N/H}} \approx 160$ MHz). We are currently investigating the origin of this fine structure.

We performed DFT calculations on both **1** and **2**.^[5] The geometries of the optimized DFT structures match quite well with the X-ray structures of **1** and **2** (*tbp* geometry for **1**, *sqpy* geometry for **2**). The HOMO of **1** and the SOMO of **2** both consist mainly of an iridium d orbital, with bonding contributions of the ethene π^* orbital and antibonding contributions of orbitals on N3 and N4. The oxidation of **1** to **2** removes one

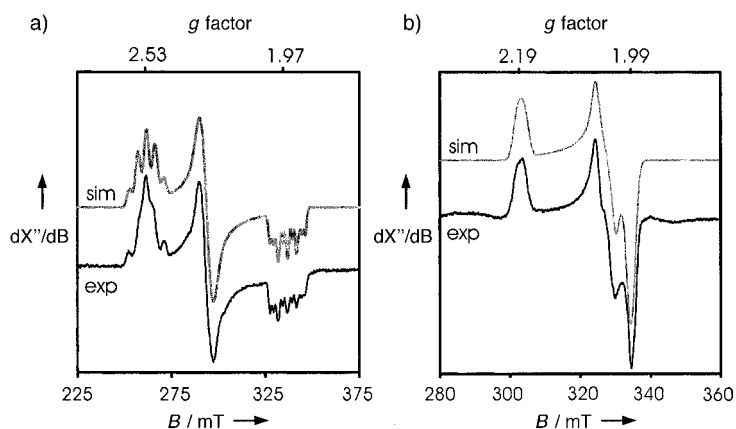


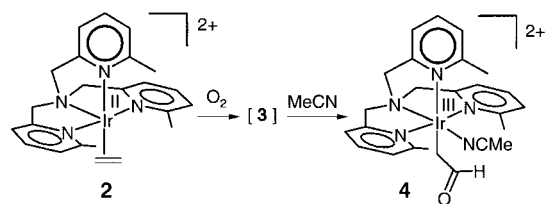
Figure 3. a) Experimental (exp) and simulated (sim) X-band EPR spectrum of **2**. b) Experimental and simulated X-band EPR spectrum of intermediate **3**. Experimental spectra in acetone:MeOH (2:3) at 40 K, 9.30 GHz. (attn. 30 dB, mod. 4 G).

electron from the HOMO of **1** to give the SOMO of **2** (see Supporting Information, Figure S1). As a result, the Ir→ethene π backbonding decreases and the Ir1–N3/Ir1–N4 σ interaction increases on going from **1** to **2**. Actually, we observe that only the Ir1–C1 distance increases and only the Ir1–N3 distance decreases (Table 1), this is because Ir1–C2 in **1** is already long as a result of steric hindrance by the axial Py-Me substituents, whereas Ir1–N4 in **1** is already short as a result of geometrical constraints by the κ^4 -Me₃-tpa ligand.

Mononuclear complexes of Rh^{III}[6] and particularly Ir^{III}[7] are rare. Most examples are stabilized by bulky dianionic porphyrinate ligands (por²⁻). To our knowledge, only one stable mononuclear Ir^{II}-olefin complex has been reported, [(C₆Cl₅)₂Ir^{II}(cod)] (cod = Z,Z-1,5-cyclooctadiene).[8] Complex **2** is the first example of a stable M^{II}-ethene (M = Rh, Ir) complex.

Recently, [(por)M^{II}(ethene)] (M = Rh,^[6] Ir,^[9] por²⁻ = a bulky meso-tetra-arylporphyrinate dianion), formed in situ from [(por)M^{II}] and ethene, have been reported to undergo bimolecular C–C radical coupling to butylene-bridged dinuclear complexes. Quite remarkably, complex **2** does *not* dimerize by radical coupling of the ethene carbon atoms. Nevertheless, the DFT calculations suggest that the coordinated ethene fragment may still have some radical character (see Supporting Information, Figure S1 and S2).

The radical character of **2** seems to be reflected in its reactivity towards O₂. Upon exposure of a solution of **2** in MeCN, acetone, or acetone:MeOH (2:3) to air or O₂ at –10 °C, the color of the solution changed from brown to purple. Upon warming these solutions to ambient temperature, the purple color vanishes, the solutions became colorless, and the ¹H NMR spectrum indicated the formation of diamagnetic products. The main product in MeCN (~70% based on ¹H NMR spectroscopy) was identified as formylmethyl^[10] complex **4** (Scheme 2). In acetone other types of products were detected. The nature of these products and the apparent solvent dependency of their formation are currently under investigation.



Scheme 2. Oxidation of **2** by O₂ yielding **4** via intermediate **3**.

The Ir^{II}-ethene complex **2** thus seems capable of O₂ activation and C–O bond formation. In marked contrast, oxidation of Ir^I-ethene complex **1** with O₂ in solution did *not* result in C–O bond formation, but yielded the peroxo-ethene complex [(κ^3 -Me₃-tpa)Ir^{III}(O₂)(C₂H₄)]⁺.^[2]

The initial color change from brown to purple in the conversion of **2** into **4** at –10 °C indicates the formation of an intermediate (**3**). The EPR spectrum of **3** is shown in Figure 3b.^[11] Simulation of the rhombic spectrum yields

$g_{11} = 1.987$, $g_{22} = 2.030$, and $g_{33} = 2.191$. The line shape for g_{22} suggests a small iridium hyperfine coupling ($A_{22}^{\text{Ir}} \approx 38$ MHz). Thus, on going from **2** to **3** a marked decrease in anisotropy of the EPR signal is observed (Figure 3). This effect might indicate a shift in spin density from the metal center to a coordinated superoxy or superoxyethyl radical.

We have thus synthesized the unique Ir^{II}-ethene complex **2** through the one-electron oxidation of Ir^I-ethene complex **1**. The radical character of **2** may be responsible for the facile C–O bond formation in this complex upon contact with O₂. The observed reactivity of **2** towards O₂ points to a possible role of Ir^{II}-olefin and Rh^{II}-olefin species in rhodium- and iridium-catalyzed oxidation of olefins by O₂. This insight is of importance in the development of catalytic olefin oxygenation by Group VIII metal centers.

Experimental Section

NMR spectroscopic experiments were carried out on a Bruker DPX200 spectrometer. X-band EPR spectra were recorded on a Bruker ER220 spectrometer. Mass Spectra were recorded on a MAT 900 XL mass spectrometer. All procedures were performed under N₂ using standard Schlenk techniques unless indicated otherwise. Compound **1**-PF₆ was prepared as reported in ref. [2]

2-(PF₆)₂: Complex **1**-PF₆ (230 mg, 0.33 mmol) was added to a solution of [Fc]PF₆ (86 mg, 0.26 mmol) in CH₂Cl₂ (12 mL). The resulting green/brown mixture was stirred for 30 min at room temperature. The resulting brown precipitate was collected by filtration. Yield 186 mg (0.221 mmol, 85%; analytically pure). Deep brown/black crystals of **2**-(PF₆)₂, suitable for X-ray diffraction, were obtained at 10 °C from a solution of the above precipitate in acetone layered with hexane. Yield after crystallization: 72 mg (0.085 mmol, 33%). ESI⁺-MS: m/z 276.5 [$M - (PF_6)_2$]²⁺, 698 [$M - PF_6$]⁺; elemental analysis calcd (%) for C₂₃H₂₈N₄IrP₂F₁₂: C 32.78, H 3.35, N 6.65; found: C 32.64, H 3.33, N 6.67.

4-(PF₆)₂: Exposure of a solution of **2**-(PF₆)₂ in MeCN to O₂ leads to a mixture of ~70% **4**-(PF₆)₂ and ~30% of yet unidentified products. From this mixture **4**-(PF₆)₂ was characterized. ¹H NMR (200 MHz, CD₃CN, 298 K): δ = 9.44 (t, 1H, ³J(H,H) = 4.55 Hz, IrCH₂C(=O)H), 7.81 (t, 2H, Py^A-H4, ³J(H,H) = 7.6 Hz), 7.69 (t, 1H, Py^B-H4, ³J(H,H) = 7.6 Hz), 7.40–7.10 (m, 6H, Py^{A/B}-H3/5), 5.32 (d[AB], 2H, ²J(H,H) = 16.4 Hz, N-CH₂-Py^A), 4.90 (d[AB], 2H, ²J(H,H) = 16.4 Hz, N-CH₂-Py^B), 3.55 (d, 2H, ³J(H,H) = 4.55 Hz, IrCH₂C(=O)H), 3.18 (s, 3H, CH₃-Py^B), 2.96 (2, 3H, Ir-NCCH₃), 2.82 ppm (s, 6H, CH₃-Py^A); ¹³C{¹H} NMR (50 MHz, CD₃CN, 298 K): δ = 208.5 (IrCH₂C(=O)H), {166.0, 164.4, 163.4, 159.3 (Py^{A/B}-C2, Py^{A/B}-C6)}, 141.3 (Py^B-C4), 140.7 (Py^A-C4), 128.6 (Py^B-C3), 128.2 (Py^A-C3), 122.7 (Py^B-C5), 120.4 (Py^A-C5), 74.9 (N-CH₂-Py^A), 71.4 (N-CH₂-Py^B), 27.3 (Py^B-CH₃), 27.2 (Py^A-CH₃), 10.4 (Ir-CH₂C(=O)H), 5.6 ppm (Ir-NCCH₃) (Ir-NCCH₃ signal obscured by solvent signal); FT-IR (KBr): $\tilde{\nu}$ = 2848, 2733 (C–H of CH=O), 1676 (C=O of CH=O), 825, 556 cm^{–1} (P–F); ESI⁺-MS (sample prepared in CD₃CN): m/z 306 [$M - (PF_6)_2$]²⁺, 284 [$M - (PF_6)_2 - CD_3CN$]²⁺, 757 [$M - PF_6$]⁺.

Received: January 31, 2002 [Z18624]

- a) B. de Bruin, J. A. Brands, J. J. M. Donners, M. P. J. Donners, R. de Gelder, J. M. M. Smits, A. W. Gal, A. L. Spek, *Chem. Eur. J.* **1999**, 5, 2921–2936; b) B. de Bruin, M. J. Boerakker, J. A. W. Verhagen, R. de Gelder, J. M. M. Smits, A. W. Gal, *Chem. Eur. J.* **2000**, 6, 298–312; c) R. J. N. A. M. Kicken, PhD thesis, University of Nijmegen (The Netherlands), **2001**; d) M. Krom, R. G. E. Coumans, J. M. M. Smits, A. W. Gal, *Angew. Chem.* **2001**, 113, 2164–2166; *Angew. Chem. Int. Ed.* **2001**, 40, 2106–2108.
- B. de Bruin, T. P. J. Peters, J. B. M. Wilting, S. Thewissen, J. M. M. Smits, A. W. Gal, *Eur. J. Inorg. Chem.*, submitted.
- Single crystals of **1**-PF₆ and **2**-(PF₆)₂ were sealed in a glass capillary under N₂. Intensity data were collected on an Enraf-Nonius CAD4 diffractometer, using graphite monochromatized MoK α radiation

($\lambda = 0.71073 \text{ \AA}$). Data were collected at room temperature ($\omega/2\theta$ -scan mode). For both compounds, unit-cell dimensions were determined from the angular setting of 25 reflections. Intensity data were corrected for Lorentz and polarization effects. Semiempirical absorption correction (ψ -scan)^[3a] was applied. For **1**-PF₆, this procedure by itself was not adequate enough. The difference Fourier map still showed peaks up to 3.6 e \AA^{-3} close to the Ir atom. Therefore an additional absorption correction was applied using the DIFABS procedure,^[3b] resulting in final residual peaks up to 2.3 e \AA^{-3} . The structures were solved by the program system DIRDIF^[3c] using the program PATTY^[3d] to locate the heavy atoms, and were refined with standard methods (refinement against F^2 of all reflections with SHELXL-97^[3e] with anisotropic parameters for the non-hydrogen atoms. The hydrogen atoms were initially placed at calculated positions, refined isotropically in riding mode, and were subsequently refined freely. For **1**-PF₆, based on geometrical considerations alone, the unit cell could be transformed to an orthorhombic C-cell ($a = 9.1795(19)$, $b = 46.2562(78)$, $c = 11.5840(17) \text{ \AA}$), but this transformation is not supported by the symmetry of the data ($R_{\text{int}} = 0.549$) nor by the unit-cell contents. From the anisotropic thermal displacement parameters for the PF₆ moieties of **2**-(PF₆)₂, it is clear that some atoms show a large positional disorder. Although it is possible to use several partially occupied positions for these atoms, no physically reasonable models result from these parameters, at least not any that are better than the models presented here. Summary of the crystal data for **1**-PF₆: (C₂₃H₂₈N₄PF₆Ir, $M_r = 697.66$): monoclinic, space group $P2_1/c$, $a = 9.1802(19)$, $b = 11.5828(18)$, $c = 23.581(4) \text{ \AA}$, $\beta = 101.193(19)^\circ$, $V = 2459.7(7) \text{ \AA}^3$, $Z = 4$, $\rho_{\text{calc}} = 1.884 \text{ g cm}^{-3}$. Final R indices: $R_1 = 0.0529$ (for 3815 reflections considered observed [$I > 2\sigma(I)$]), $wR_2 = 0.1314$ (all data) for the 319 total variables. Summary of the crystal data for **2**-(PF₆)₂: (C₂₃H₂₈N₄P₂F₁₂Ir, $M_r = 842.63$): monoclinic, space group $P2_1/a$, $a = 13.072(2)$, $b = 12.454(2)$, $c = 18.860(3) \text{ \AA}$, $\beta = 109.734(11)^\circ$, $V = 2890.0(8) \text{ \AA}^3$, $Z = 4$, $\rho_{\text{calc}} = 1.937 \text{ g cm}^{-3}$. Final R indices: $R_1 = 0.0393$ (for 5292 reflections considered observed [$I > 2\sigma(I)$]), $wR_2 = 0.1011$ (all data) for the 382 total variables. a) A. C. T. North, D. C. Philips, F. S. Mathews, *Acta Crystallogr. Sect. A* **1968**, *24*, 351; b) N. Walker, D. Stuart, *Acta Crystallogr. Sect. A* **1983**, *39*, 158; c) P. T. Beurskens, G. Beurskens, W. P. Bosman, R. de Gelder, S. Garcia-Granda, R. O. Gould, R. Israel, J. M. M. Smits, DIRDIF-96, A computer program system for crystal structure determination by Patterson methods and direct methods applied to difference structure factors; Crystallography Laboratory, University of Nijmegen (The Netherlands), **1996**; d) P. T. Beurskens, G. Beurskens, M. Strumpel, C. E. Nordman in *Patterson and Pattersons* (Eds.: J. P. Glusker, B. K. Patterson, M. Rossi), Clarendon, Oxford, **1987**, p. 356; e) G. M. Sheldrick, SHELXS-97, Program for the refinement of crystal structures, University of Göttingen, Göttingen (Germany), **1997**. CCDC-176107 for **1**-PF₆ and CCDC-176108 for **2**-(PF₆)₂ contains the supplementary crystallographic data for this paper. These data can be obtained free of charge via www.ccdc.cam.ac.uk/conts/retrieving.html (or from the Cambridge Crystallographic Data Centre, 12, Union Road, Cambridge CB2 1EZ, UK; fax: (+44) 1223-336-033; or deposit@ccdc.cam.ac.uk).

- [4] Organic π radicals normally show much weaker superhyperfine coupling with H nuclei, e.g. C₂H₅⁺ radical: 70 MHz; allyl free radical: 11–42 MHz; naphthalene anion radical: 5–13 MHz. B. H. J. Bielski, J. M. Gebicki, *Atlas of Electron Spin Resonance Spectra*, Academic Press, New York, **1967**.
- [5] Geometries were optimized at the B3LYP level^[12] by using the Gaussian98 suite of programs.^[13] Basis sets used include the LANL2DZ basis and pseudo potential^[14] for the iridium center and STO3G^[15] on all other atoms. The orbitals presented here were visualized using the Molden program (see Supporting Information).^[16]
- [6] D. G. DeWit, *Coord. Chem. Rev.* **1996**, *147*, 209–246, and references therein.
- [7] K. K. Pandey, *Coord. Chem. Rev.* **1992**, *121*, 1–42, and references therein.
- [8] M. P. Garcia, M. V. Jimenez, L. A. Oro, F. J. Lahoz, P. J. Alonso, *Angew. Chem.* **1992**, *104*, 1512–1514; *Angew. Chem. Int. Ed. Engl.* **1992**, *31*, 1527–1529.
- [9] H. L. Zhai, A. Bunn, B. Wayland, *Chem. Commun.* **2001**, 1294–1295.
- [10] Other formylmethyl M^{III} species (M = Rh, Ir) have been reported: a) D. Milstein, J. C. Calabrese, *J. Am. Chem. Soc.* **1982**, *104*, 3773–

- 37741; b) B. de Bruin, J. A. W. Verhagen, C. H. J. Schouten, A. W. Gal, D. Feichtinger, D. A. Plattner, *Chem. Eur. J.* **2001**, *7*, 416–422; c) M. Krom, R. G. E. Coumans, J. M. M. Smits, A. W. Gal, *Angew. Chem.* **2002**, *114*, 595–599; *Angew. Chem. Int. Ed.* **2002**, *41*, 576–579.
- [11] During conversion of **2** into **3** at -10°C in acetone:MeOH (2:3) some decomposition of **3** occurs. At approximately 50% conversion, **3** was present in about 40% of the initial spin concentration. At full conversion, **3** was present in around 30% of the initial spin concentration. Attempts to record EPR spectra of **2** and **3** in MeCN yielded very broad spectra, probably because of the poor quality of the MeCN glass and/or crystallization. However, despite the broadness of the signals, aerated samples of **2** in MeCN show EPR peaks at the same positions as those for **2** and **3** in acetone:MeOH (2:3).
- [12] a) A. D. Becke, *J. Chem. Phys.* **1993**, *98*, 5648–5652; b) C. Lee, W. Yang, R. G. Parr, *Phys. Rev. B* **1988**, *37*, 785–789; c) B. Miehlich, A. Savin, H. Stoll, H. Preuss, *Chem. Phys. Lett.* **1989**, *157*, 200–206.
- [13] Gaussian98 (Revision A.7), M. J. Frisch, G. W. Trucks, H. B. Schlegel, G. E. Scuseria, M. A. Robb, J. R. Cheeseman, V. G. Zakrzewski, J. A. Montgomery, R. E. Stratmann, J. C. Burant, S. Dapprich, J. M. Millam, A. D. Daniels, K. N. Kudin, M. C. Strain, O. Farkas, J. Tomasi, V. Barone, M. Cossi, R. Cammi, B. Mennucci, C. Pomelli, C. Adamo, S. Clifford, J. Ochterski, G. A. Petersson, P. Y. Ayala, Q. Cui, K. Morokuma, D. K. Malick, A. D. Rabuck, K. Raghavachari, J. B. Foresman, J. Cioslowski, J. V. Ortiz, B. B. Stefanov, G. Liu, A. Liashenko, P. Piskorz, I. Komaromi, R. Gomperts, R. L. Martin, D. J. Fox, T. Keith, M. A. Al-Laham, C. Y. Peng, A. Nanayakkara, C. Gonzalez, M. Challacombe, P. M. W. Gill, B. G. Johnson, W. Chen, M. W. Wong, J. L. Andres, M. Head-Gordon, E. S. Replogle, J. A. Pople, Gaussian, Inc., Pittsburgh, PA, **1998**.
- [14] a) W. J. Hehre, R. F. Stewart, J. A. Pople, *J. Chem. Phys.* **1969**, *51*, 2657–2664; b) J. B. Collins, P. v. R. Schleyer, J. S. Binkley and J. A. Pople, *J. Chem. Phys.* **1976**, *64*, 5142–5151.
- [15] a) P. J. Hay, W. R. Wadt, *J. Chem. Phys.* **1985**, *82*, 270–283; b) W. R. Wadt, P. J. Hay, *J. Chem. Phys.* **1985**, *82*, 284–298; c) P. J. Hay, W. R. Wadt, *J. Chem. Phys.* **1985**, *82*, 299–310.
- [16] G. Schaftenaar, J. H. Noordik, *J. Comput.-Aided Mol. Des.* **2000**, *14*, 123–134.


A Highly Regioselective Synthesis of Polysubstituted Naphthalene Derivatives through Gallium Trichloride Catalyzed Alkyne–Aldehyde Coupling**

Ganapathy S. Viswanathan, Mingwen Wang, and Chao-Jun Li*

Polysubstituted aromatic compounds have played an important role in the chemical and pharmaceutical industries as well as in the fields of optical and electronic materials. Traditionally, the regioselective construction of polysubstituted aromatic compounds has been carried out by the stepwise introduction of substituents through electrophilic substitutions.^[1] More modern achievements in the regioselective

[*] Prof. Dr. C.-J. Li, G. S. Viswanathan, Dr. M. Wang
Department of Chemistry, Tulane University
New Orleans, LA 70118 (USA)
Fax: (+1) 504-865-5596
E-mail: cjli@tulane.edu

[**] This work has been partially supported by the US NSF CAREER Award program and the US NSF-EPA STAR program.

 Supporting information for this article is available on the WWW under <http://www.angewandte.org> or from the author.